Stability analysis of a new Passive PMs Bearing

Ernesto Tripodi [a], Antonino Musolino [a], Rocco Rizzo [a], Dante Casini [a]

[a] Department of Energy and System Engineering, University of Pisa, Largo Lucio Lazzarino, I-56126 Pisa, Italy, ernesto.tripodi@dsea.unipi.it

***Abstract*—In this paper a new Permanent Magnets (PMs) bearing is presented. The device is composed of a rotor capable to levitate at a short distance from a dedicated stator. The magnetic suspension is achieved by proper configurations of PMs arranged on both the stator and the rotor. The device is characterized by intrinsic instability and passive stabilization is attempted exploiting eddy currents on a conducting sheet surrounding the stator magnets. The system has been simulated by means of a dedicated numerical tool capable to take into account the effects of the magneto-mechanical coupling. In particular, the coupled problem has been integrated by means of a prediction-correction nested scheme. The simulation activity has produced some interesting results, that are here extensively discussed. More specifically, it has been shown that the stability with respect to the center of mass translation can be passively obtained, if the rotations are actively prevented. An idea of an active stabilizing system for the rotations, exploiting the results of the simulation is finally briefly described.**

I. Introduction

The modern development of Magnetic Levitation systems (known as MAGLEV) started in the late 1960s, when the idea of using magnetic force to levitate vehicles became bearable, mainly due to some recent discoveries: the development of low-temperature superconducting wire, the transistor and chip based electronic control technology [1], [2]. MAGLEV provides high-speed motion, safety, reliability, low environmental impact and minimum maintenance [3]. There are two basic options to obtain magnetic levitation: electromagnetic system [4], [5], [6] working in attraction mode with forces generated by electromagnets and electrodynamic system [7], [8] working in repulsive mode with forces generated by superconductive coils. Both the solutions are characterized by unstable behavior. In particular the first one is unstable in the levitating direction (typically vertical): in fact as the two parts of the systems approach one the other the attractive force increases. The electrodynamic system is unstable in the direction transverse to levitation and in the motion directions. The nowadays availability of rare heart PMs (e.g. NdFeB) characterized by high values of remnant field has made possible to conceive a new class of MAGLEV systems where the suspension is assured by the repulsion of properly shaped PMs [9], [10]. As known, stability of levitation systems based on PMs is prevented by Earnshaw's theorem [11]. This theorem states that a set of steady charges, magnetizations, or currents cannot stay in stable equilibrium under the action of stady electric and magnetic field alone. Several applications of MAGLEV or magnetic bearing devices must be fail-safe, and this poses severe constraints on the design and operation of the stabilization systems. In this context a great effort is devoted to the design of passive and more reliable stabilization devices. There are some circumstances under which electric and magnetic systems can avoid the consequences of the Earnshaw's theorem: time varying fields (e.g., eddy currents, alternating gradient), active feedback, ferrofluids, superconductors and diamagnetic systems. In this paper, the use of eddy current stabilization for the reduction or the elimination of the intrinsic instability of the bearing is investigated. More precisely, if some magnetized parts of a system are in motion near conductive materials, eddy currents are induced and the system is not under the action of steady magnetic fields alone. The hypothesis of the Earnshaw's theorem, that is a direct consequence of the Laplace equation, is not valid in this case since the system is now governed by the diffusion equation. In this paper some preliminary results of the coupled electromechanical analysis of a PMs bearing are discussed, showing how the presence of motional induced eddy currents have a positive effect on the dynamic of the bearing device, so reducing the complexity of the control system. In particular, Section II introduces the proposed device, Section III briefly describes the numerical tool used for the analysis of the device, while Section IV discusses the obtained results. In Section V the results obtained are summarised and a simple control system is proposed to achieve the overall stability.

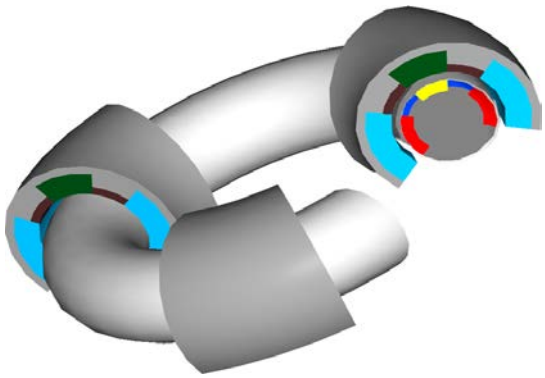

Figure 1. A 3D view of the analysed device.

II. Proposed Device

The proposed system, exploiting the induced eddy currents to contrast the instability related to the PMs arrangement is shown in figures 1 and 2. It is composed of a toroidal stator and a segmented rotor made of (at least) three blocks equally spaced along the circumference. The stator is fixed while the rotor can move with 6 degrees of freedom (DoFs).

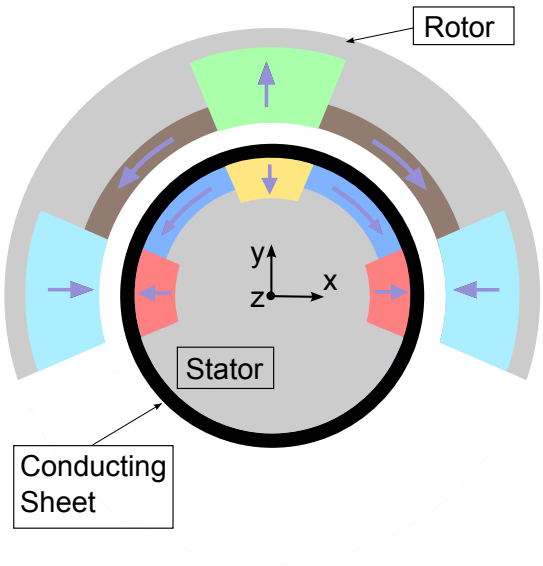

Figure 2. Cross section of the bearing.

The PMs in both the stator and the rotor are arranged in Halbach array configurations [12] focusing the field lines in the airgap between them. A sheet of conductive material surrounds the stator (black in 2. Levitation (along z-direction) is achieved by the repulsion of oppositely magnetized PMs. In order to describe the dynamics of the proposed device let us assume that the moving part rotates around a vertical shaft (directed as the z-axis) coincident with the symmetry axis of the stator. A system of motion induced eddy currents flows on the stator sheet; as a consequence a levitation force in the z-axis direction (which sums with the levitation force of the PMs) and a magnetic drag torque are observed. In fact, the motion induced eddy currents interact with the PMs of the rotor in order to reduce the cause that produces the eddy currents themselves. This is achieved by a velocity reduction (a drag force on the rotor) but also by moving the source of the inducing field (the PMs on the rotor) away from the conductive region. The system is stable in the levitation direction since the levitation force is a decreasing function of the distance. In correspondence to the symmetric configuration radial forces cancel. If the symmetry condition does not hold (e.g. because of a radial shift of the rotation shaft) a net force in the radial direction is expected to appear. This force is the resultant of the forces between the two PMs systems and those between the motion induced eddy currents and the PMs on the rotor. As known (Earnshaw's theorem) the forces between the PMs are destabilizing and as a consequence the rotor would touch the stator after a short time. Referring to figure 2, if we consider a displacement of the rotor in the y-axis direction we see that the currents induced on the conductive sheet are stronger on the side characterized by a reduced distance with the rotor, while are weaker on the side where the distance is greater. The net resulting force is then directed along the negative y-axis direction so performing a stabilizing action. The described stabilizing contribution of the forces between the induced currents and the PMs is present in the case of angular displacement of the rotation shaft with respect to the vertical (z-axis) direction. Considering that the rotor is segmented in at least three sectors, as a results of this angular displacement some of its sectors are closer to the stator, others more distant. The induced currents on the regions of the stator which correspond to the nearest sectors of the rotor are more intense and consequently the forces exerted on the PMs in these sectors of the rotor are strongest. On the contrary the forces on the rotor sectors that are more distant from the stator are decreased. The resultant effect is a torque restoring the vertical position of the rotation shaft.

III. The Numerical Electromechanical Formulation

In order to investigate the performance of this system it is necessary to use a numerical model. The equations describing the rotor dynamics with six DoFs are inherently nonlinear because of the dependence of the force on the position of the rotor itself. Moreover the dynamic problem is coupled with the diffusion equation of the magnetic field. The solution of the electromagnetic problem has been carried out by an integral formulation that reduces the diffusion equation to an equivalent network with time varying parameters. The values of the parameters in the electrical equations are function of the position of the rotor. The details of the adopted formulation are reported in [13], [14] and the development of a C code exploiting the GPGPU Nvidia CUDA libraries is extensively described in [15].
Under the hypothesis of linear magnetisable materials the equations of the problem produced by the equivalent network formulation coupled with the Newton-Euler equations of motion, can be written as:

$$\begin{aligned} &\mathbf{L}\left(\mathbf{C}\left(t\right)\right)\frac{d\mathbf{i}}{dt}+\left[\mathbf{R}\left(\mathbf{C}\left(t\right)\right)+\mathbf{K}\left(\mathbf{C}\left(t\right),\dot{C}\left(t\right)\right)\right]\mathbf{i}=\mathbf{e}(t)\\ &\mathbf{F}\left(\mathbf{C}\left(t\right)\right)=m\ddot{\mathbf{q}}\\ &\mathbf{M}\left(\mathbf{C}\left(t\right)\right)=\mathbf{I}_{\theta\theta}\dot{\boldsymbol{\omega}}+\boldsymbol{\omega}\times\mathbf{I}_{\theta\theta}\boldsymbol{\omega}\end{aligned} \tag{1}$$

where $\mathbf{e}(t)$ represents the vector of the applied voltage generators and $\mathbf{i}$ is the vector of the currents in the elementary volumes, included the equivalent magnetization currents. All the coefficients matrices are function of which represents the system configuration at the instant t. $\mathbf{C}(t)$ is defined as the set of the positions and orientations of all the elementary volumes in which the device is discretized:

$$\mathbf{C}\left(t\right)=\left(\mathbf{x}\left(t\right),\mathbf{y}\left(t\right),\mathbf{z}\left(t\right),\boldsymbol{\phi}\left(t\right),\boldsymbol{\theta}\left(t\right),\boldsymbol{\psi}\left(t\right)\right)$$

$\mathbf{L}\left(\mathbf{C}\left(t\right)\right)$ denotes the inductance matrix; $\mathbf{R}\left(\mathbf{C}\left(t\right)\right)$ is the resistance matrix and $\mathbf{K}\left(\mathbf{C}\left(t\right),\dot{\mathbf{C}}\left(t\right)\right)$ takes into account the electromotive force due to the motional effects. In particular $\dot{\mathbf{C}}(t)$, termed as the derivatives of the system configuration at the instant t, describes the velocity of every elementary volume in the hypothesis of rigid body. The $\dot{\mathbf{C}}_i(t)$ corresponding to the i-th elementary volume is constituted by the three components of the translation velocity, the three components of the angular velocity, and the three coordinates of the center of rotation.
Equation (1) is solved by a prediction correction nested scheme. The rationale behind it is the search for an approximation of the time dependence of the coefficients in

electrical and mechanical equations. The predictor-corrector approach is used to obtain an approximate behavior of the named quantities by a linear interpolation between the known values at the previous time step and the predicted values at the next time step. Inserting this knowledge in the equations has the effect of considering updated values of the coefficients, allowing a coupling between the equations which is stronger than the one in a simply staggered scheme and comparable with a monolithic approach. The integration algorithm can be described as follows ($\Delta t = t_{n+1} - t_n$):

- assuming $\mathbf{C}(t)$ constant in the interval Δt an estimate of the currents at t_n is obtained by a trapezoidal rule applied on (1a);
- an estimate of $\mathbf{C}\left(t_{n+1}\right) = \mathbf{C}_{n+1}$ is obtained by applying forward Euler integration to (1b) and (1c);
- a piecewise linear approximation is assumed for $\mathbf{L}$ in Δt, similarly for $\mathbf{R}$ and $\mathbf{K}$:

$$\dot{\mathbf{L}}\left(t_n\right) \simeq \frac{\mathbf{L}\left(\tilde{\mathbf{C}}\left(t_{n+1}\right)\right) - \mathbf{L}\left(\tilde{\mathbf{C}}\left(t_n\right)\right)}{\Delta t}$$

and so

$$\mathbf{L}(t) \simeq \mathbf{L}\left(t_n\right) + \dot{\mathbf{L}}\left(t_n\right) \cdot \left(t - t_n\right) = \mathbf{L}_n + \dot{\mathbf{L}}_n \cdot \left(t - t_n\right);$$

- The expressions are introduced in (1a):

$$\left(\mathbf{L}_n + \dot{\mathbf{L}}_n \cdot \left(t - t_n\right)\right) \frac{d\mathbf{i}}{dt} + \left[\left(\mathbf{R}_n + \dot{\mathbf{R}}_n \cdot \left(t - t_n\right)\right) + \left(\mathbf{K}_n + \dot{\mathbf{K}}_n \cdot \left(t - t_n\right)\right)\right] \mathbf{i} = \mathbf{e}(t) \quad t \in [t_n,\, t_{n+1}] \tag{2}$$

- integrating with a trapezoidal-like rule we obtain the corrected values of the currents at the instant t_{n+1}. We write:

$$\int_{t_n}^{t_{n+1}} \left(\mathbf{L}_n + \dot{\mathbf{L}}_n \left(t - t_n\right)\right) \frac{d\mathbf{i}}{dt} dt + \int_{t_n}^{t_{n+1}} \left[\left(\mathbf{R}_n + \dot{\mathbf{R}}_n \left(t - t_n\right)\right) + \left(\mathbf{K}_n + \dot{\mathbf{K}}_n \left(t - t_n\right)\right)\right] \mathbf{i} dt = \int_{t_n}^{t_{n+1}} \mathbf{e}(t) dt \tag{3}$$

- and after the numerical integration:

$$\mathbf{L}_n \left(\mathbf{i}_{n+1} - \mathbf{i}_n\right) + \frac{\Delta t \dot{\mathbf{L}}_n}{2} \left(\mathbf{i}_{n+1} + \mathbf{i}_n\right) + \frac{\Delta t \left(\mathbf{R}_n + \mathbf{K}_n\right)}{2} \left(\mathbf{i}_{n+1} + \mathbf{i}_n\right) + \frac{\Delta^2 t \left(\dot{\mathbf{R}}_n + \dot{\mathbf{K}}_n\right)}{2} \mathbf{i}_{n+1} = \frac{\Delta t \left(\mathbf{e}_{n+1} + \mathbf{e}_n\right)}{2} \tag{4}$$

- Collecting terms finally gives a linear system where the unknowns are the corrected currents at the instant t_{n+1} :

$$\left(\mathbf{L}_n + \frac{\Delta t \dot{\mathbf{L}}_n}{2} + \frac{\Delta t \left(\mathbf{R}_n + \mathbf{K}_n\right)}{2} + \frac{\Delta^2 t \left(\dot{\mathbf{R}}_n + \dot{\mathbf{K}}_n\right)}{2}\right) \mathbf{i}_{n+1} = = \frac{\Delta t \left(\mathbf{e}_{n+1} + \mathbf{e}_n\right)}{2} + \left(\mathbf{L}_n - \frac{\Delta t \dot{\mathbf{L}}_n}{2} - \frac{\Delta t \left(\mathbf{R}_n + \mathbf{K}_n\right)}{2}\right) \mathbf{i}_n \tag{5}$$

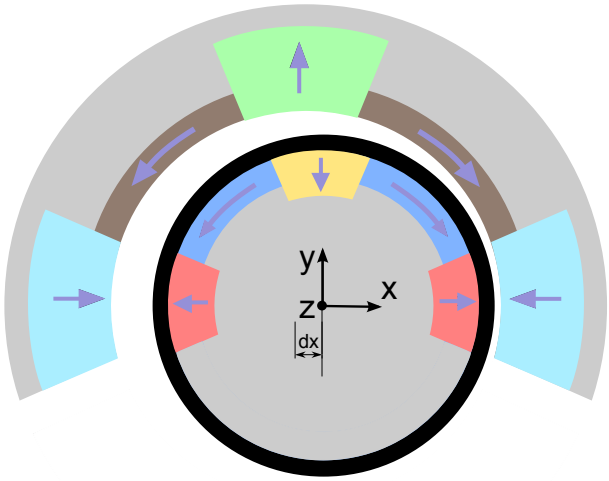

Figure 3. Configuration with the rotor shifted along the x-axis.

- Once (5) is solved, force and torque are evaluated again by using the force coefficient in the predicted configuration $\tilde{\mathbf{\Phi}}\left(t_{n+1}\right)$ with the corrected values of the currents $\mathbf{i}\left(t_{n+1}\right)$ just obtained. The integration of the mechanical equations yields the corrected position of the moving body.

The integration method has been validated and the results exhibit a very good accuracy respect to the experimental data found in literature, as [16].

IV. Simulation Results

As a case study we considered a device with an average radius of 8 cm. The tube constituting the stator has a radius of 2.2 cm and the clearance between rotor and stator is 7 mm. We made a set of simulations driving the rotor at different rotational speeds. We noticed that, at low speeds (less than 3000 rpm), the stabilizing effect was not enough (i.e. the system behavior was really close to the static case, without enough levitation force), while, increasing the speed over a certain value (more than 4000 rpm) have the effect of reducing the magnetic drag force, as expected, but without significative variations in the stabilizing effect. We report here the results obtained with a rotational speed of 4800 rpm.

The levitation force at rest is 450 N and increases to 470 N at motion. The radial magnetized red and blue sectors have an angle of 67.50°, the green and yellow an angle of 45° while the azimuth magnetized purple and pink sectors have an angle of 33.75°. The radial width is 0.5 cm for the red and yellow sectors, 1 cm for the green and blue, and 0.3 cm for the purple and pink ones. The thickness of the conductive (aluminum) sheet is 2mm. The numerical formulation in Section III has been used to perform the analysis of some configurations obtained by the described device.

We started considering the device with the conductive sheet removed with an initial position characterized by the rotation shaft shifted of 1.5 mm with respect to the symmetry axis as shown in figure 3. The results of simulation are shown in figures 4 and 5. As expected the system is unstable with

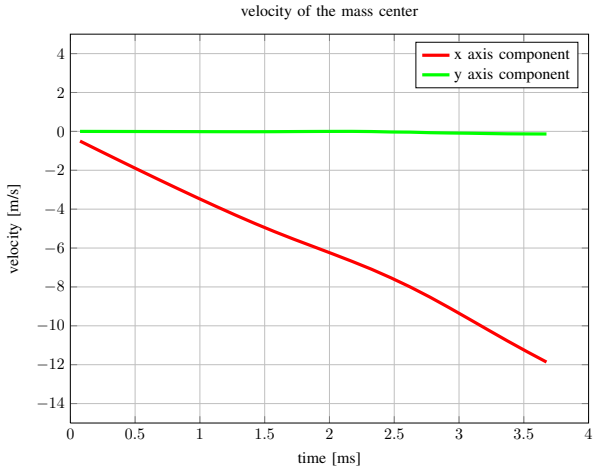

Figure 4. Velocity of the center of mass of the rotor.

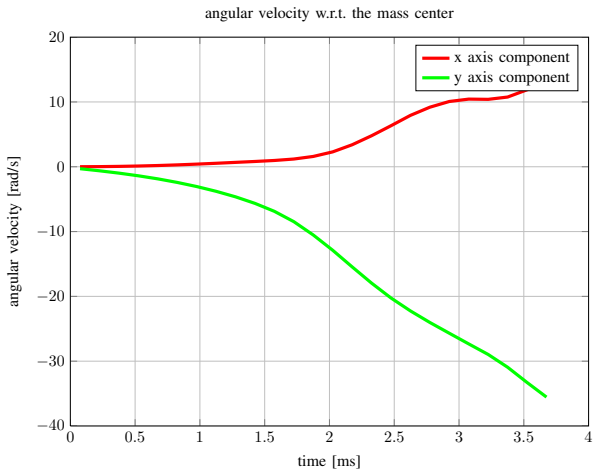

Figure 5. Components of the angular velocity.

respect to the radial direction and with respect the rotation around the x and the y axes. The contact between the rotor and the stator happens after about 3 ms. Figures 6 and 7 refer to the configuration where the conductive sheet has been introduced. Also in this case the rotor touches the stator as a consequence of the unstable behavior of the system. We can observe that the presence of the conductive sheet (and of the induced currents) is able to slower the unstable dynamics; the rotor takes a longer time (about 17 ms) to touch the stator.

Despite the eddy currents on the sheet are not able to stabilize the device, they can be used to reduce the complexity of the control system since a lower dynamic requires a slower control action that is easier to be designed. To further investigate the effects of the currents on the conductive sheet we performed simulations of the device with a reduced number of DoFs preventing rotations respect to x and y axes assuming the presence of two of the mentioned bearings arranged in a vertical configuration. Figure 8 shows the velocity waveforms while figure 9 shows the force waveforms; the simulation has been done with the same lateral displacement $dx = 1.5$ mm.

According to the results of the simulation, the dynamic of the system is stable. This is actually a good result if we think

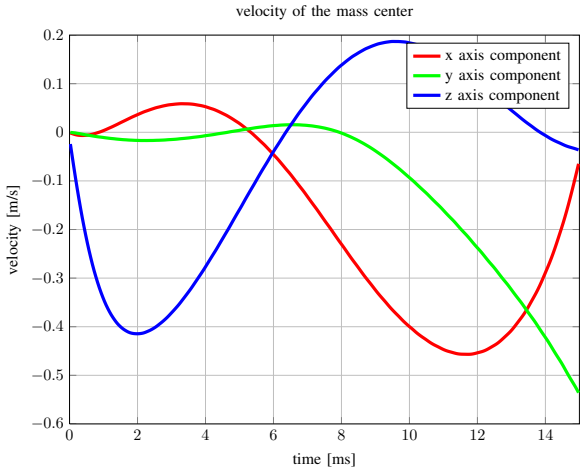

Figure 6. Velocity of the center of mass of the rotor.

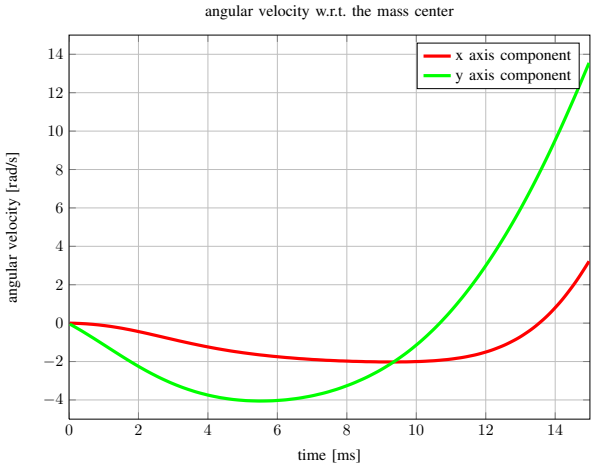

Figure 7. Components of the angular velocity.

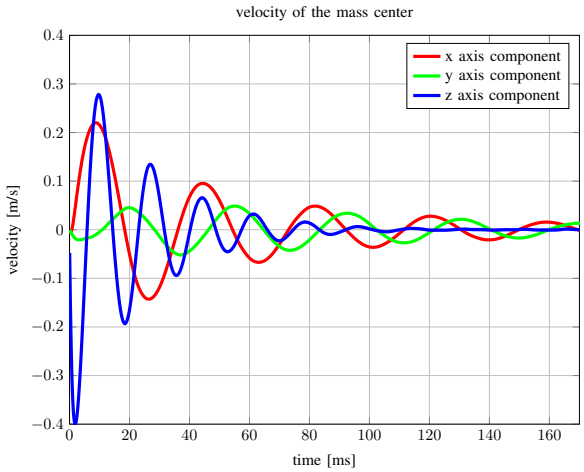

Figure 8. Velocity of the center of mass of the rotor with 3 DoFs.

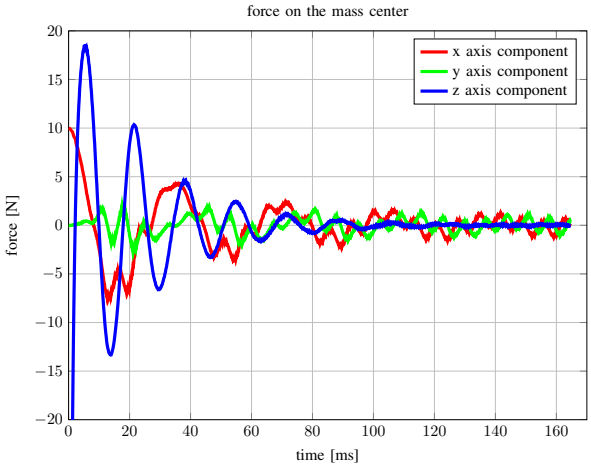

Figure 9. Force the center of mass of the rotor with 3 DoFs.

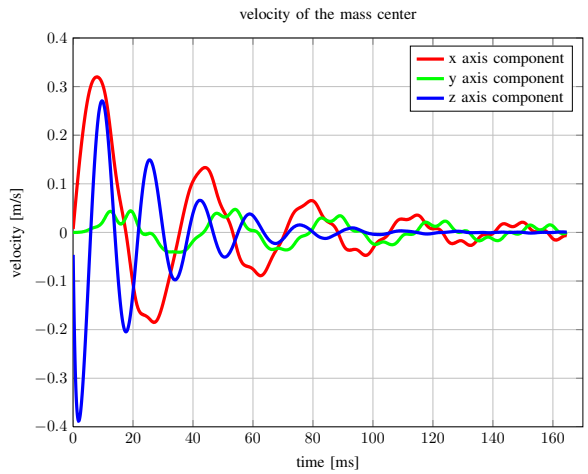

Figure 10. Velocity of the center of mass of the rotor with 3 DoFs.

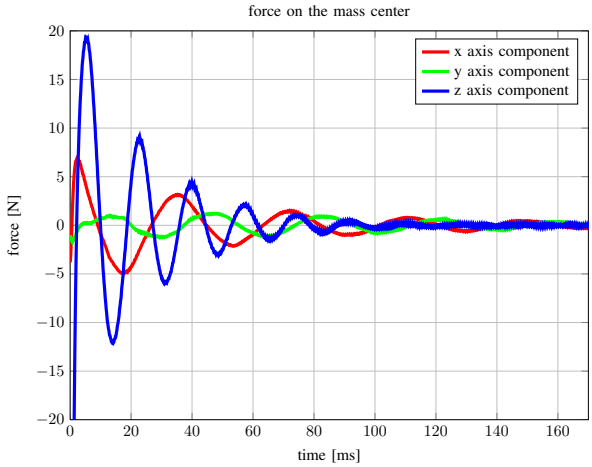

Figure 11. Forces on the center of mass of the rotor with 3 DoFs.

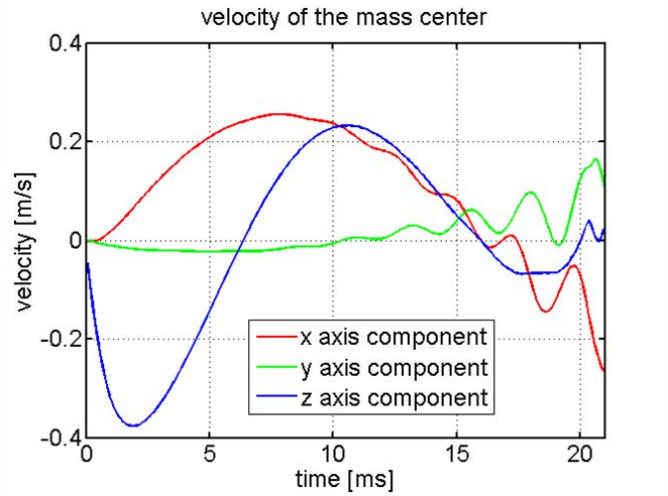

Figure 12. Velocity of the center of mass of the rotor.

that in this kind of devices, stability has to be discussed in the contest of dynamics. This means that the robustness requirements previously mentioned, involve concepts of dynamic stability in presence of modeling error due to uncertainties (modern non linear dynamics). This theory, usually, not only requires the knowledge of how the forces and torques change with the position and orientation but also of how they changes with both linear and angular velocities. The control systems are consequently usually really complex: this result is then really interesting because it permits a simpler synthesis of the active controller and so reducing the cost. Another similar simulation has been done applying a lateral force of 10 N to the rotor. The results are shown in figures 10 and 11; the system is able to compensate the lateral force as well as for the lateral displacement.

We finally performed a simulation (6 DoFs) where only the vertically magnetized PMs (the yellow and the green ones in figure 2) are retained in the stator. The results are reported in figs. 12 and 13 respectively for the velocities, while in fig.14 for what concerns the forces on the center of mass. The system remains unstable, but its response has changed showing an oscillatory behavior. The contact occurs after 22 ms. The levitation force has about halved.

V. Conclusions

An exhaustive simulation activity has been performed on a PMs bearing based on Halbach array configurations. The conductive sheet is not sufficient to stabilize to system, but it makes slower the unstable dynamics, actually simplifying the control systems action. Since the actuators basically consist of coils, a slower dynamics will need slower control actions, and then smaller voltages. The main result of the our analysis relies in the intrinsic stability with respect to the mass center translation, once the rotations with respect x and y axes are prevented. This means that a stabilization system is needed only to maintain the direction of the rotation axis parallel to the z-axis, while the system is able to stabilize the position of the rotation axis. Equivalently, if the stabilizing action results in a net force beside the needed torque, the system is able to compensate this force by adjusting it position. A possible setup for a stabilization device is shown in figure 15, where four electromagnets are positioned in each side of the rotating shaft where some ferromagnetic material has been inserted.

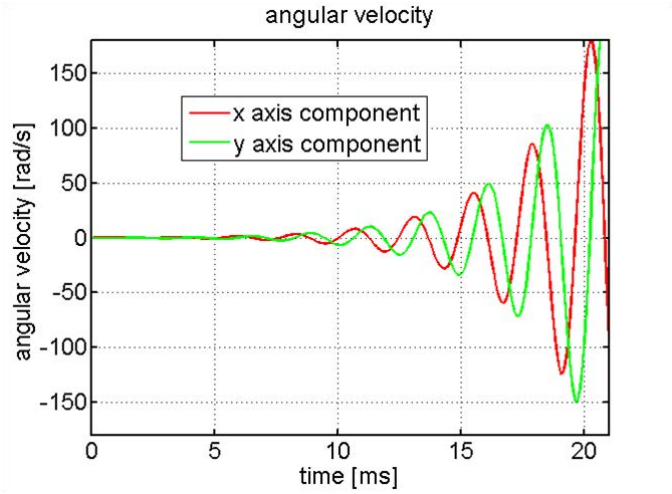

Figure 13. Components of the angular velocity.

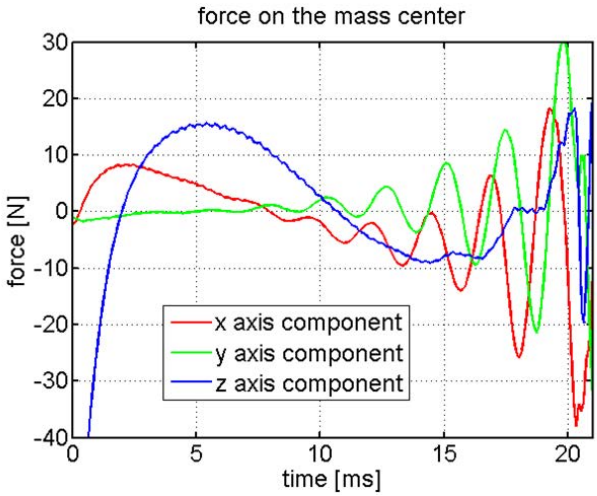

Figure 14. Forces on the center of mass of the rotor with 3 DoFs.

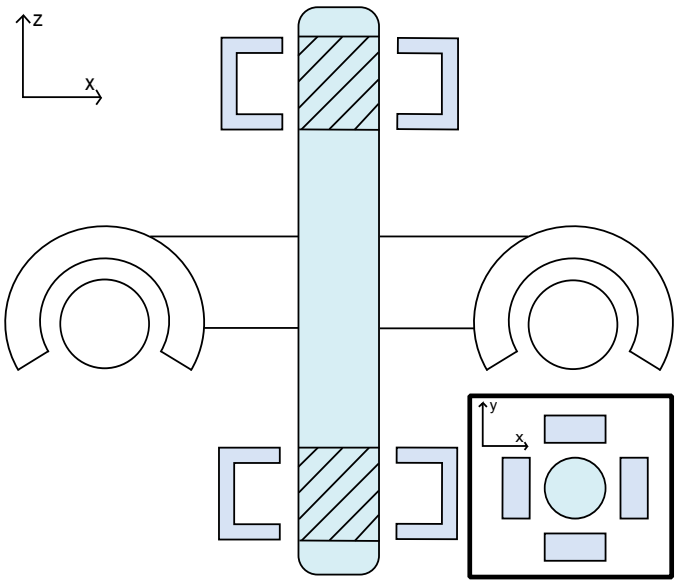

Figure 15. Components of the angular velocity.

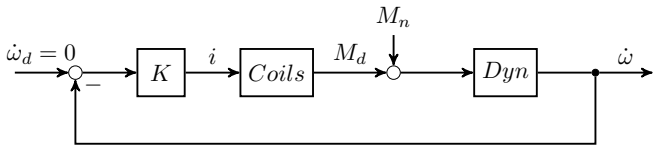

Figure 16. Control scheme.

The current in the coils of the electromagnets can be controlled by the value of the angular acceleration, as in the simple control scheme shown in figure 16.

References

[1] V. Kozorez and O. Cheborin, "On stability of equilibrium in a system of two ideal current rings," in *Dokl. Akad. Nauk UkrSSR, Ser. A*, vol. 4, 1988, pp. 80–81.

[2] F. C. Moon, *Chaotic and Fractal Dynamics: Introduction for Applied Scientists and Engineers*. John Wiley & Sons, 2008.

[3] H.-W. Lee, K.-C. Kim, and J. Lee, "Review of maglev train technologies," *Magnetics, IEEE Transactions on*, vol. 42, no. 7, pp. 1917–1925, 2006.

[4] J. Meins, L. Miller, and W. Mayer, "The high speed maglev transport system transrapid," *Magnetics, IEEE Transactions on*, vol. 24, no. 2, pp. 808–811, 1988.

[5] N. Amati, A. Tonoli, F. Impinna, and J. Girardello Detoni, "A solution for the stabilization of electrodynamic bearings: Modeling and experimental validation," *Journal of Vibration and Acoustics*, vol. 133, pp. 021 004–1, 2011.

[6] A. Tonoli, N. Amati, F. Impinna, J. G. Detoni, H. Bleuler, and J. Sandtner, "Dynamic modeling and experimental validation of axial electrodynamic bearings," in *Proceedings of the 12th International Symposium on Magnetic Bearings*, 2011, p. 68.

[7] M. Ono, S. Koga, and H. Ohtsuki, "Japan's superconducting maglev train," *Instrumentation & Measurement Magazine, IEEE*, vol. 5, no. 1, pp. 9–15, 2002.

[8] E. Diez-Jimenez, J.-L. Perez-Diaz, and J. C. Garcia-Prada, "Local model for magnet–superconductor mechanical interaction: Experimental verification," *Journal of Applied Physics*, vol. 109, no. 6, pp. 063 901–063 901, 2011.

[9] N. Paudel, J. Z. Bird, S. Paul, and D. Bobba, "Modeling the dynamic suspension behavior of an eddy current device," in *Energy Conversion Congress and Exposition (ECCE), 2011 IEEE*. IEEE, 2011, pp. 1692–1699.

[10] A. Musolino, R. Rizzo, M. Tucci, and V. M. Matrosov, "A new passive maglev system based on eddy current stabilization," *Magnetics, IEEE Transactions on*, vol. 45, no. 3, pp. 984–987, 2009.

[11] S. Earnshaw, "{On the nature of the molecular forces which regulate the constitution of the luminiferous ether}," *Trans. Camb. Phil. Soc*, vol. 7, pp. 97–112, 1842.

[12] K. Halbach, "Application of permanent magnets in accelerators and electron storage rings," *Journal of Applied Physics*, vol. 57, no. 8, pp. 3605–3608, 1985.

[13] A. Musolino, R. Rizzo, M. Toni, and E. Tripodi, "Acceleration of electromagnetic launchers modeling by using graphic processing units," in *Electromagnetic Launch Technology (EML), 2012 16th International Symposium on*. IEEE, 2012, pp. 1–6.

[14] A. Musolino and R. Rizzo, "Numerical modeling of helical launchers," *Plasma Science, IEEE Transactions on*, vol. 39, no. 3, pp. 935–940, 2011.

[15] A. Musolino, R. Rizzo, E. Tripodi, and M. Toni, "Modeling of electromechanical devices by gpu-accelerated integral formulation," *International Journal of Numerical Modelling: Electronic Networks, Devices and Fields*, vol. 26, no. 4, pp. 376–396, 2013.

[16] H. Karl, J. Fetzer, S. Kurz, G. Lehner, and W. M. Rucker, "Description of team workshop problem 28: an electrodynamic levitation device," in *Proceedings of the TEAM Workshop in the Sixth Round*. Citeseer, 1997, pp. 48–51.